Assessing strain rate sensitivity of cement paste at the micro-scale through micro-cantilever testing

Gan, Yidong; Rodriguez, Claudia Romero; Schlangen, Erik; van Breugel, Klaas; Šavija, Branko

DOI
10.1016/j.cemconcomp.2021.104084

Publication date
2021

Document Version
Final published version

Published in
Cement and Concrete Composites

Cement and Concrete Composites 121 (2021) 104084

Contents lists available at ScienceDirect

Cement and Concrete Composites

journal homepage: www.elsevier.com/locate/cemconcomp

Assessing strain rate sensitivity of cement paste at the micro-scale through micro-cantilever testing

Yidong Gan *, Claudia Romero Rodriguez, Erik Schlangen, Klaas van Breugel, Branko Šavija

Microlab, Faculty of Civil Engineering and Geosciences, Delft University of Technology, Delft, 2628, CN, the Netherlands

ARTICLE INFO

Keywords:
Strain rate sensitivity
Micro-cantilever bending
Cement paste
Creep

ABSTRACT

This study presents an experimental investigation of the rate-dependent mechanical properties of cement paste at the microscale. With the use of a nanoindenter, micro-cantilever beams with the size of 300 μm × 300 μm × 1650 μm were loaded at five different strain rates from around 10^{-6}/s to 10^{-2}/s until failure. It is found that with increasing strain rate, the stress-strain curves show less and delayed pre-peak nonlinearity. Both the flexural strength and the elastic modulus of beams increase with increasing strain rate, while the strain at peak stress exhibits an opposite trend. Examination of the fracture surface indicates that with increasing strain rate the possibility of a crack to pass through stronger components of the hydration products is increased. The experimental observations and possible mechanisms leading to changes in mechanical responses are discussed. It is suggested that at least two micromechanical processes, namely creep and Stéfan effect, are mainly responsible for the rate-dependent behaviour of cement paste within the investigated strain rate range and their dominances seem to vary with the strain rate. At lower strain rate, the strain rate sensitivity of cement paste is thought to be dominated by the creep effect, while at higher strain rate the Stéfan effect appears to be the governing factor.

1. Introduction

Concrete structures encounter a wide range of loading rates in practice, ranging from a slowly applied load to impact loads and blast [1–3]. It is well known that the mechanical properties of concrete are sensitive to the strain rate [4–8]. However, this strain rate effect has not been fully understood yet, partly because the concrete is a complicated composite. Since cement paste is the main binding component of concrete, the knowledge regarding its rate-dependent mechanical properties will help to understand the corresponding behaviour of mortar and concrete. As suggested by many researchers [9–14], the strain rate sensitivity of cementitious material is strongly associated with several micromechanical processes. Therefore, it is necessary to investigate the strain rate sensitivity of cement paste at the microscale.

Even though extensive studies have been dedicated to the rate-dependent behaviour of cementitious materials, there are not many studies focusing on the rate dependency of cement paste at the microscale. Recently, Liang et al. [12] used the microindentation technique to investigate the strain rate sensitivity of cement paste at the microscale. They found that the contact hardness of cement paste increases with the increasing strain rate. However, the strain rate sensitivity of the strength cannot be directly extracted from the conventional indentation technique [15,16]. Alternatively, the recent development of small-scale testing approach for characterizing the fracture properties of miniaturized samples [15–22,63–65] offers an opportunity to assess the strain rate sensitivity of strength at the microscale. In this novel experimental approach, the miniaturized samples, with a size from 100 μm to 500 μm, are generated by using a precise micro-dicing saw. Afterwards, by using the nanoindenter as the loading instrument, the load-displacement response of the sample is measured until failure. Various types of microscale tests, e.g. micro-cantilever bending tests [20,22], compressive tests [17] and one-side splitting tests [21,23], have been performed to investigate the corresponding flexural, compressive and splitting strength of cement paste at the microscale. So far, all these tests have been conducted under quasi-static loading conditions and the strength at lower or higher strain rate has not been experimentally examined. In the current paper, the micro-cantilever bending method is adopted to investigate the strain rate sensitivity of mechanical properties of cement paste.

In the literature, various mechanisms have been proposed to explain

* Corresponding author.
E-mail addresses: y.gan@tudelft.nl (Y. Gan), C.RomeroRodriguez@tudelft.nl (C.R. Rodriguez), Erik.Schlangen@tudelft.nl (E. Schlangen), K.vanBreugel@tudelft.nl (K. van Breugel), B.Savija@tudelft.nl (B. Šavija).

https://doi.org/10.1016/j.cemconcomp.2021.104084
Received 8 May 2020; Received in revised form 14 January 2021; Accepted 28 April 2021
Available online 1 May 2021

the rate-dependent behaviour of cementitious materials, such as the creep related damage [9,10,24,25], Stéfan effect [7,13,26,27], inertia effect [1,28,29] and rate-dependent crack propagation [11,28]. It has been generally recognized that several physical processes could occur simultaneously, but which process is dominant mainly depends on the magnitude of the strain rate. When strain rate changes from very low (i.e. $<10^{-6}$/s) to very high (i.e. $>10^{1}$/s), the governing mechanism is thought to vary from the creep effect to inertia effect and rate-dependent cracking propagation [9,14,27]. However, in contrast to the apparent distinction between those two extreme strain rate cases, a thorough and unambiguous understanding of rate-dependent behaviour at intermediate rates is still missing. Therefore, additional research on this strain rate range is needed.

This paper aims to investigate the strain rate effect on the mechanical properties of cement paste at the microscale and to improve the understanding of the involved micromechanical processes under the intermediate strain rates. The micro-cantilever beams (MCB) with the size of 300 μm × 300 μm × 1650 μm were first prepared using the micro-dicing saw technique. These beams were then subjected to bending tests with the aid of nanoindenter. Two w/c ratios with five different strain rates were examined in this study. The strain rate sensitivity was measured in terms of flexural strength, elastic modulus and strain at peak stress. Special attention has also been paid on the possible rate-dependent cracking process by means of the microscopic observation on the fracture surface and X-ray computed tomography scanning of the beam before and after failure. General discussions regarding the strain rate mechanisms of cement paste in the investigated strain rate range are also provided.

2. Materials and methods

2.1. Materials and experimental procedure

2.1.1. Materials

The materials used in this study were standard grade CEM I 42.5 N Portland cement (ENCI, Netherlands) and deionized water. The Blaine fineness of cement is 284 m^2/kg reported by the manufacturer. Two water/cement ratios (0.3 and 0.4) were used for cement paste. The pastes were first cast in plastic cylindrical moulds with 24 mm diameter and 39 mm height. To mitigate the influence of bleeding, the fresh paste was rotated at a speed of 2.5 rpm for one day at room temperature (26 °C). The samples were cured under sealed conditions at room temperature for 28 days. After demoulding, the hardened cement pastes were cut into 3 mm thick slices. The slices were then immersed in isopropanol to arrest the hydration [30].

2.1.2. Preparation of micro-cantilever beams

Micro-cantilever beams (MCB) were prepared using a precision micro-dicing machine (MicroAce Series 3 Dicing Saw), which is generally used to cut semiconductor wafers. The first step in this sample preparation process was to grind the slices of cement paste to obtain two smooth and parallel surfaces. In the grinding process, two grinding discs of 135 μm and 35 μm were used in sequence. Once the thickness of 2.15 mm was reached, two perpendicular cutting directions with the same cutting space were applied on the samples using the micro-dicing machine. In this way, multiple rows of cantilever beams with a square cross section of 300 μm × 300 μm were generated. The cutting depth, i.e. the cantilevered length, was approximately 1650 μm ± 10 μm. The cutting process is schematically shown in Fig. 1. The cross-sections of several randomly selected beams were examined by using an Environmental Scanning Electron Microscope (ESEM). No cracking resulting from the specimen preparation process was observed. An overall accuracy of the cross-sectional dimensions of ±1.5 μm can be reached with this fabrication process (Fig. 2). Precautions were also taken to minimize the carbonation of the samples before testing by storing the beams in isopropanol.

2.2. Micro-cantilever bending test

A KLA Nano indenter G200 was used to perform bending tests with different loading rates on the MCBs. The baseplate was first attached on a metal surface using cyanoacrylate adhesive. A cylindrical wedge indenter tip (Fig. 3) with a length of 200 μm was used to apply vertical line loads at the free end of the beams. Before testing, the angle and centre of the tip are always calibrated by probing into a standard aluminium reference sample. Afterwards, the angle of MCB is carefully adjusted under the in-situ microscope in the nanoindenter to ensure that

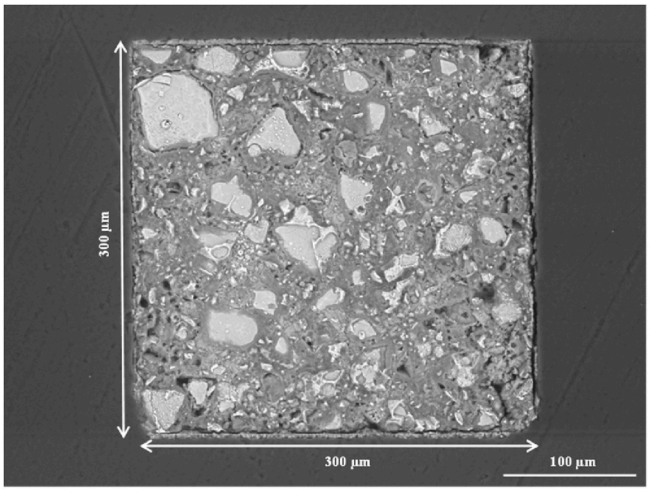

Fig. 2. Backscattered electron image of the cross-sections of cantilever beam [36].

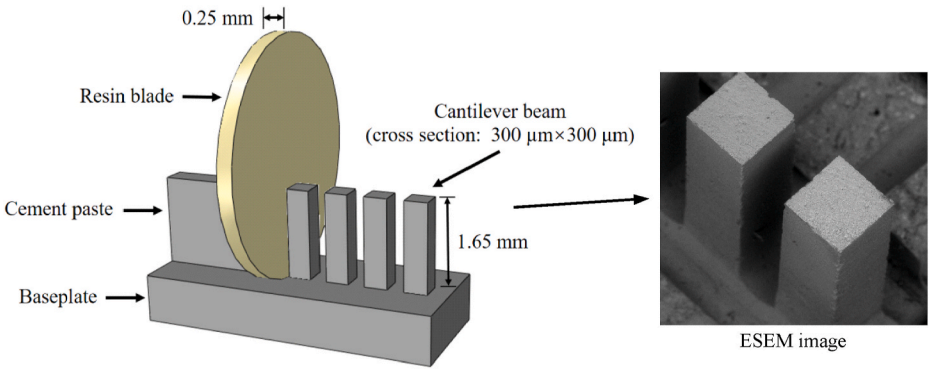

Fig. 1. Schematic diagram of sample preparation [22].

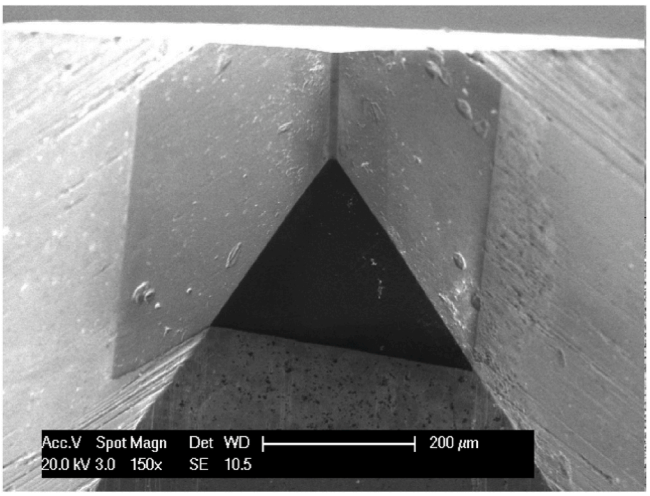

Fig. 3. Secondary electron image of the diamond cylindrical wedge tip [36].

the line load is applied perpendicularly to the beam longitudinal axis. The experimental set-up is schematically shown in Fig. 4. For each test the coordinates of the loading position and the fixed end were recorded under the microscope to determine the loading length. All beams were then monotonically loaded to failure. In general, a major crack will initiate near the fixed end during the loading, which will eventually lead to complete fracture of the beam. After failure of the beam, the coordinates of the fracture point were also recorded.

In this study, the MCBs were loaded at five displacement rates, ranging from around 4.1 nm/s to over 50,000 nm/s. Successive displacement rates were increased by approximately one order of magnitude. The corresponding strain rates at the upper fibre of the fixed end of beams are used to interpret the results. It should be mentioned here that due to the technical limitation of the employed nanoindenter, the tests with the slowest strain rate were carried out under load control, while the rest of strain rate tests were controlled by displacement. As long as the load-displacement response is almost linear and only the pre-peak behaviour is concerned, which seems to be the case in this study (see Fig. 5a), the two testing protocols are expected to provide similar response. Nevertheless, the rate of displacement for each test was recorded and averaged. The calculated average strain rates for w/c 0.3 samples ranged from 1.3 με/s to 4.3×10^3 με/s. For the w/c 0.4 samples, the average strain rates were from 0.7 με/s to 5.0×10^3 με/s. Fig. 5b shows the typical load-displacement curves for w/c 0.3 samples under different strain rates. Note that the failure is always accompanied with an overshoot of the indenter tip resulting in a rapid burst of displacement (Fig. 5a and b), which appears to be a nearly brittle fracture. It may also be that the nanoindenter is not fast enough to capture the post-peak behaviour of the specimen. Nevertheless, the meaningless data points

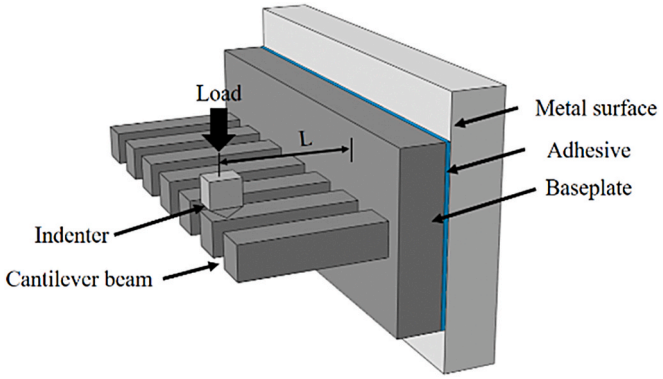

Fig. 4. Schematic diagram of test set-up.

after failure have been removed and only the pre-peak (including the maximum load) curves are presented and analysed in the following sections.

At the slowest strain rate, MCBs failed in around 1 h, while at the fastest strain rate they failed in less than 0.3 s. The sampling rate of data acquisition ranged from 5 Hz (the slowest tests) to 500 Hz (the fastest test). For each strain rate, 30 cantilever beams were tested to provide a good level of statistical confidence. All tests were conducted in a well-insulated chamber preventing any significant change of temperature and RH. The average temperature and RH during the tests were 26.8 ± 0.6 °C and 33.2% ± 0.5%, respectively. Before each test, the samples were kept in the chamber for temperature equalization until the thermal drift rate was below 0.05 nm/s. To gain more information regarding the fracture process under different strain rates, several MCBs were also scanned using X-ray micro computed tomography (XCT) before and after failure (see Fig. 6). The micro-cantilever beams were fixed on the glass holders for XCT experiment, see Fig. 6 (a). A gold mark on one side of the glass holder was used to locate the loading surface of the beam. The X-ray tube was set at 90 kV/170 μA for the scanning. The obtained voxel resolution was $1.3 \times 1.3 \times 1.3$ μm^3/voxel.

3. Results

3.1. Stress-strain curves

Since there is always a small variation of loading distance in different tests, it is more appropriate to present the stress-strain curves instead of the load-displacement curves. The stress (σ) and strain (ε) at the upper fibre of the fixed end can be calculated based on the classical beam theory:

$$\sigma = \frac{FLh}{2I} \tag{1}$$

$$\varepsilon = \frac{3\delta h}{2L^2} \tag{2}$$

where F is the load, L is the measured distance between the load point and the fixed end, h is the side length of the square cross-section, $I = h^4/12$ is the moment of inertia, and δ is the measured displacement of the indenter tip. The typical stress-strain curves for cement pastes with different w/c ratios and loading rates are shown in Fig. 7. One should bear in mind that due to the highly heterogeneous nature of cement paste at microscale, the stress-strain response of samples may largely differ even under identical testing condition. Overall, the slope of the stress-strain curve and the maximum stress tend to increase with increasing strain rate for the two w/c ratios. Moreover, there is an apparent difference between the highest strain rate test and the rest of strain rate tests. At first glance, all the stress-strain relationships are almost linear suggesting a possible linear elastic behaviour of cement paste at the microscale. However, a closer look at the end of curves (lower-right) reveals that there is a small deviation from linearity (dash line) for lower strain rate tests. The observed pre-peak nonlinearity also tends to show less and later with increasing strain rate. When the strain rate is higher than 10^{-4}/s, this pre-peak nonlinearity is hardly observed. This observation is similar with the findings in macroscopic tests on concrete [4,6,11,26,31]. For the slowest strain rate tests under load control, a consequence of such a loading regime is that several jumps in strain corresponding to the onset of microcracking were observed. These measured local discontinuities imply that the damage evolution (i.e. initiation and propagation of microcracks) might occur inside the beams at higher stress level. This is also in analogy to the fracture behaviour of concrete that before the maximum strength is reached, the microcracks first develop in a diffuse manner [26]. Note that the representative size of a macrocrack in cement paste at the microscale should be substantially smaller than that of concrete at the macroscale. It seems that the increased strength at higher strain rate may be due to less accumulation

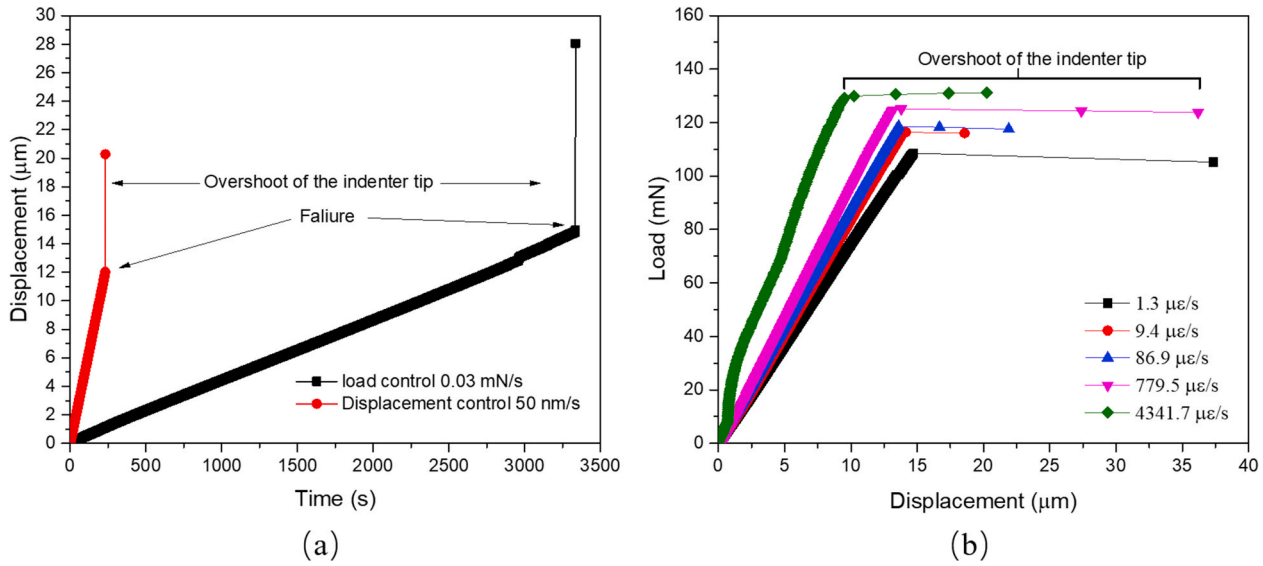

Fig. 5. (a) Typical time-displacement curves; (b) typical load-displacement curves for five strain rates.

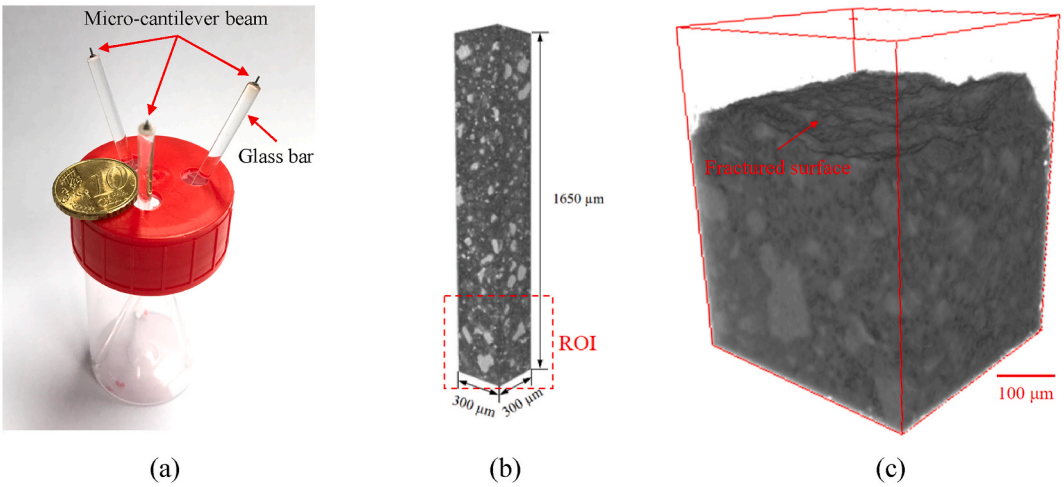

Fig. 6. Schematic view of XCT experiment: (a) micro-cantilever beam fixed on the glass holder for CT scanning; (b) selecting the region of interest; (c) fractured beam.

of microcracks [4,26]. It needs to be mentioned here that not all the beams under slow strain rate exhibited the same non-linear behaviour as several beams also showed almost completely linear behaviour until failure. This is believed to be mainly dependent on the local microstructure at the fixed end of beam, in particular the tension zone, where a large portion of connected capillary pores may lead to an instant fracture once the crack is initiated.

Turning now to the results of the highest strain rate tests (the green line in Fig. 7), a sudden increase of slope can be observed at the initial part of curve. It is thought to be caused by the temporary acceleration of the indenter tip at the beginning of the fast loading regime. The initial motionless microbeam will generate the resistance to the fast change in its velocity caused by the indenter tip. This initial accelerated load results in an increased slope owing to the inertia effect. At later stage, this effect quickly vanished as the predefined constant loading speed is reached.

3.2. Flexural strength

The flexural strengths of the MCBs were calculated using the measured maximum loads according to Equation (1). Note that the measured distance between the loading point and the fracture point was used, and not the nominal length of the cantilever beam. Since some large entrapped air voids (>150 μm) may be randomly present inside the beams, the load bearing capacity of beam may be considerably reduced, especially when the voids are located near the fixed end. This has been confirmed by the ESEM observation of the fracture surface [22]. Therefore, these obtained extremely low strengths due to the premature failure of beams are considered as outliers and excluded from the following analysis. For the selection of outlier, two simple rules were followed, i.e. by selecting samples with mechanical properties lower than 30% of average value and final fractured lengths less than 1500 μm. The variations of averaged flexural strength with the strain rate for pastes with different w/c ratios are plotted in Fig. 8 on the semi-log scale. As is expected, the flexural strength increases with the increasing strain rate. At a given strain rate, higher w/c ratio results in lower strength. For the samples with the w/c ratio of 0.3, the flexural strength of the fastest test is 23.9% higher than that of the slowest test, while the flexural strength is increased by 18.7% for the w/c 0.4 between the fastest and slowest test. The corresponding absolute value of strength is increased by 7.03 MPa and 4.20 MPa for w/c 0.3 and 0.4, respectively. However, it is noticed that at strain rate lower than around

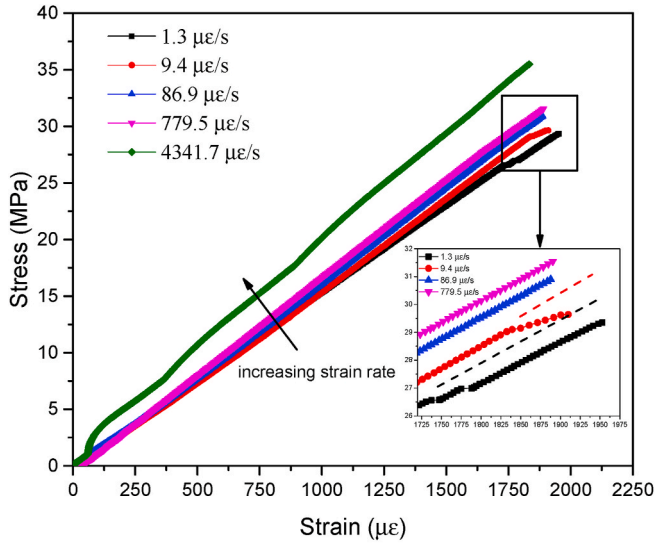

(a)

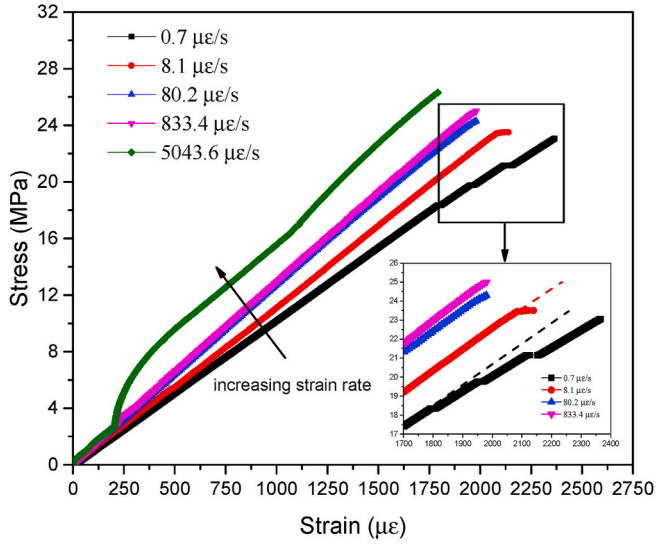

(b)

Fig. 7. Typical stress-strain curves under different strain rates for (a) w/c 0.3; (b) w/c 0.4.

10^{-5}/s, the increased absolute strength for w/c 0.4 (1.17 MPa) is higher than that of w/c 0.3 (0.39 MPa), while at higher strain rate, i.e. >0.8 × 10^{-3}/s, the opposite trend is found with larger increased strength observed in w/c 0.3 samples (3.81 MPa) compared to samples of w/c 0.4 (1.98 MPa).

For a better understanding of the stochastic fracture performance of cement paste at microscale, the Weibull statistical analysis was used to evaluate the scatter in measured flexural strength. The probability of fracture (P_f) for a two-parameter Weibull distribution can be written as [18]:

$$P_f = 1 - \exp\left[-\left(\frac{\sigma}{\sigma_0}\right)^m\right] \quad (3)$$

where m is the Weibull modulus and σ_0 is the stress corresponding to 63% probability of fracture, also known as the scaling parameter. The histograms of measured flexural strengths along with the fitted Weibull distribution for different strain rates are shown in Fig. 9. For each strain rate, a great dispersion can be seen owing to the heterogeneous nature of

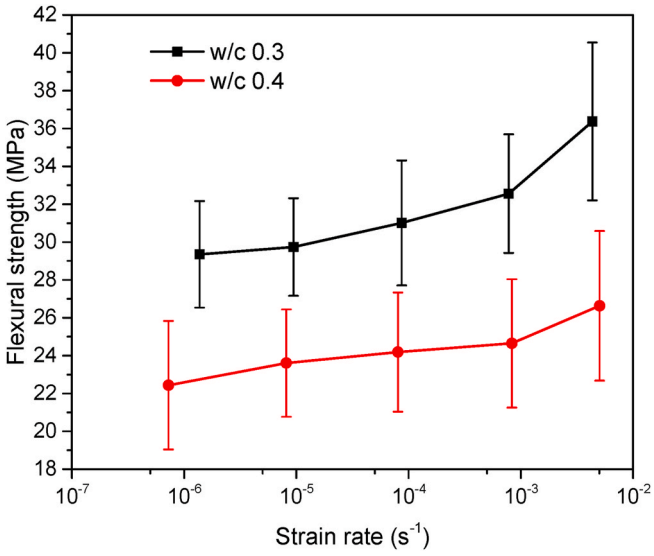

Fig. 8. The variation of flexural strength with the strain rate.

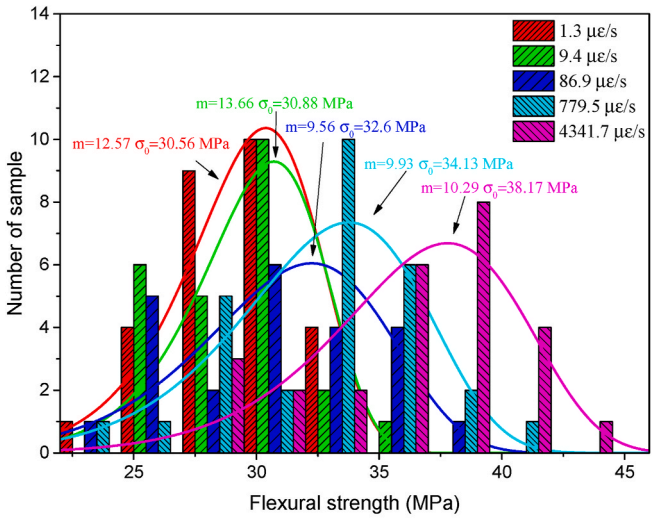

(a)

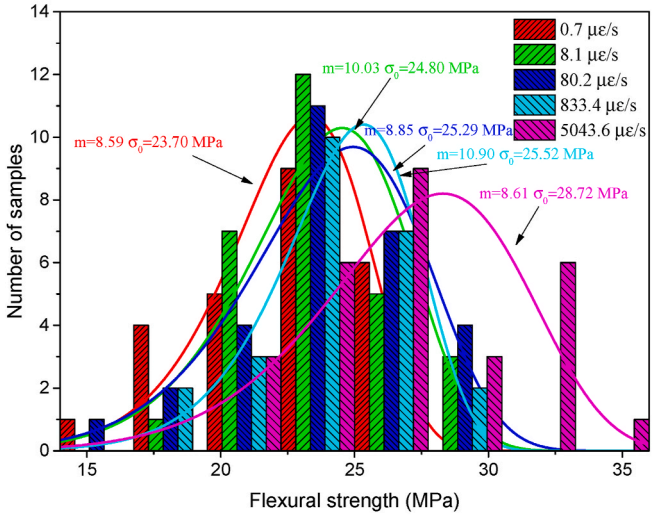

(b)

Fig. 9. The histograms of flexural strength for (a) w/c 0.3; (b) w/c 0.4.

cement paste at this scale. Apparently, with the increasing strain rate, a shift towards higher values is observed in the histograms of strengths. The results of flexural strength are then plotted in a Weibull coordinate system (Fig. 10). The least squares method was adopted to fit the Weibull modulus (m) and the scaling parameter (σ_0). A coefficient of determination (R^2) higher than 0.9 is observed for all strain rates. The obtained Weibull modulus and scaling parameter are summarized in Table 1. In general, a higher Weibull modulus indicates less scatter in the data [17,19]. It can be seen that both the Weibull modulus and scaling parameter decrease with the increasing w/c ratio. Larger variability for higher w/c ratio has also been reported in other microscale tests of cement paste in literature [15–22]. In addition, the Weibull modulus seems to be independent of the strain rate in current study. Similar findings have also been reported in macroscopic concrete tests performed by Zech and Wittmann [32].

3.3. Elastic modulus

In this study, the slope of the stress-strain curve in the range between 40% and 60% of strength was used to determine the apparent elastic modulus. This range is chosen in order to exclude the influence of the initial acceleration of the indenter tip at highest strain rate tests. In addition, the possible nonlinearity at the later stage of curves can also be avoided. Besides, since the nanoindenter records the displacement of the tip head instead of directly measuring the beam deflection, the measured total displacement may also contain the penetration depth of the indenter tip during the loading stage. The penetration depth was assessed by conducting cyclic loading on the beam and is found to be around 2%–3% of total beam deflection. For the sake of simplicity, the penetration depth is not considered in the determination of elastic modulus. Furthermore, finite element simulations [22] suggest that the deformations of the baseplate and the adhesive layer account for 14 ± 0.2% and 0.5 ± 0.1% of the total displacement, respectively. These additional displacements will be excluded from the determination of the elastic modulus. In order to validate the experimental protocol, five glass cantilever beams were fabricated and tested. The measured elastic moduli of glass beams through bending tests are 69.1 ± 1.2 GPa, which have been calibrated using the value 14.5%. For comparison, the conventional nanoindentation technique equipped with a Berkovich tip was used to measure the indentation modulus of glass (10 indents). The measured average indentation modulus is 70.1 ± 1.8 GPa, which is very close to the result obtained in bending tests. Therefore, the value

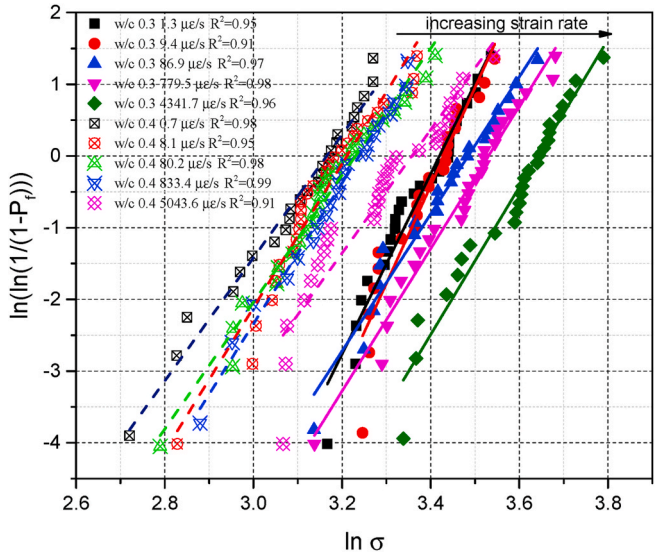

Fig. 10. The Weibull plot of the flexural strength for different strain rates and w/c ratios.

Table 1
The summary of Weibull parameters.

w/c ratio	Strain rate (με/s)	m	σ_0 (MPa)	R^2
0.3	1.3	12.57	30.56	0.95
	9.4	13.66	30.88	0.91
	86.9	9.56	32.60	0.97
	779.5	9.93	34.13	0.98
	4341.7	10.29	38.17	0.96
0.4	0.7	8.59	23.70	0.98
	8.1	10.03	24.80	0.95
	80.2	8.85	25.29	0.98
	833.4	10.90	25.52	0.99
	5043.6	8.61	28.72	0.91

(14.5%) used in the current paper is considered to be acceptable. More importantly, as pointed out by many researchers [9,33,34], the actual elastic modulus of cementitious material will always be underestimated as the displacements measured in the loading phase are not only elastic but also include some viscoelastic deformation. This creep effect becomes more significant when the slow strain rate is applied due to the extended test duration [9]. It is well known that for a purely linear viscoelastic material, the Boltzmann superposition principle can be used to estimate the viscoelastic deformation considering the loading history [9,33,35]. Herein, the cement paste is first assumed to behave in a linear viscoelastic manner during the loading process. The stress is supposed to increase monotonically at a constant stress rate. The stress history is then subdivided into a sequence of many small steps with the identical time interval. Based on the previous study of the authors on the creep behaviour of MCBs under the constant loading [36], the power-law creep compliance function was adopted. Therefore, the creep strain evolution during the monotonic loading process can be calculated in the framework of Boltzmann's superposition principle [9,33,35]:

$$\varepsilon_{creep}(t) = \sum_{i=1}^{n}[\sigma(t_i) - \sigma(t_{i-1})][\alpha(t - t_i)^{\beta}] \quad (4)$$

where $t_0 = 0$ s; α and β are two parameters of the creep compliance function [36]. According to Ref. [36], the α and β are, respectively, taken as 0.23 and 0.39 for samples with the w/c ratio of 0.3 and 0.51 and 0.39 for w/c 0.4. Since every microbeam should be different in terms of creep parameters, the effects of creep parameter variations have been examined. It is found that the overall difference due to variations of parameters is less than 1.4% for w/c 0.3 samples and 2.8% for w/c 0.4 samples. Therefore, the effect of creep parameter variations is considered to be negligible. The convolution integral of the creep compliance function and the stress history $\sigma(t)$ can produce the function for creep strain evolution $\varepsilon_{creep}(t)$ during the loading stage. Fig. 11 compares the typical stress-strain curves with or without the creep deformation. The evolution of creep strain with time is shown in the lower-right of Fig. 11. By subtracting the creep deformation from the original load-displacement curve, the time-independent stress-strain curve can be obtained. Note that since the Boltzmann's superposition principle is based on the assumption of linear viscoelasticity, the possible non-linear creep behaviour at higher stress level is not considered [9]. It has been reported that the nonlinear creep-related damage begins to increase significantly at a load level of approximately 40%–50% of strength at macroscopic tests on concrete [9,37]. However, it has been found in Ref. [36] that the cement paste (w/c 0.4) at the microscale exhibits linear viscoelastic behaviour up to around 70% of flexural strength. Therefore, in consideration of the elastic modulus, which is determined by the slope within the range of 40%–60% of strength, the assumption of the linear viscoelasticity seems to be valid for the current study.

The calculated elastic moduli with or without creep effect are plotted in Fig. 12. It can clearly be seen that the apparent elastic moduli calculated from the original stress-strain curves (solid line) are more sensitive to the strain rate than the time-independent elastic moduli

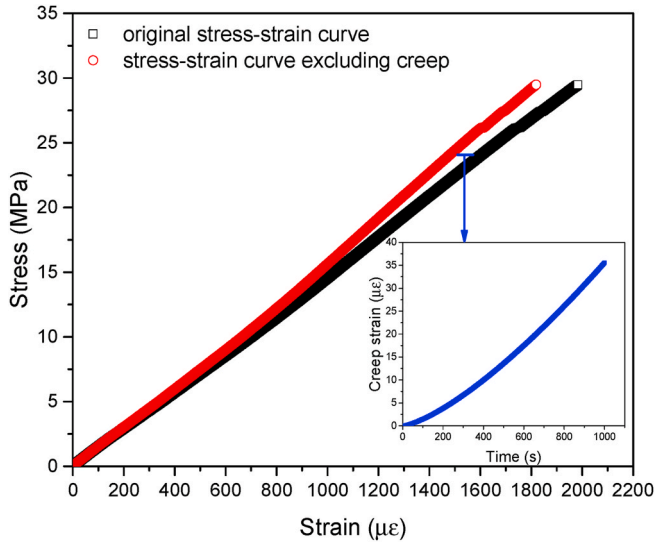

Fig. 11. The stress-strain curves with or without creep deformation.

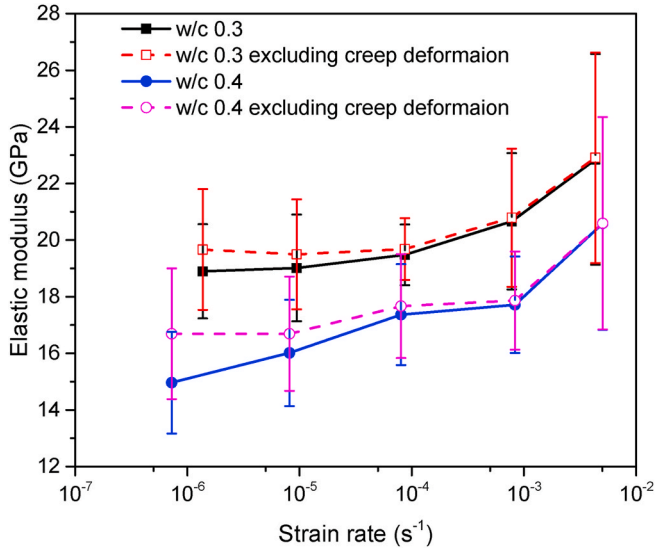

Fig. 12. The variation of elastic modulus with the strain rate.

(dash line) for low strain rates ($<10^{-3}$/s). It may imply that the dependence of elastic modulus on the strain rate is the consequence of creep at least for the strain rates lower than 10^{-3}/s. There is no doubt that for pastes with a lower w/c ratio and shorter testing duration the creep deformation is less [9,38]. At higher strain rate, the creep effect may be neglected due to the much shorter testing duration. However, a substantial increase of the time-independent elastic modulus is still observed for both w/c ratios. This indicates that there is another contributor enhancing the elastic modulus at higher strain rate [13]. The increasing percentages of apparent elastic modulus between the fastest and slowest strain rate were 21% and 37.6% for cement paste with the w/c ratio of 0.3 and 0.4, respectively, while the increasing percentages of 15.7% and 23.4% were found for the corresponding time-independent elastic modulus.

3.4. Peak strain

In this study, the peak strain is defined as the strain at the peak stress. Fig. 13 shows the variation of the average peak strain as a function of strain rate (solid line). A descending trend of peak strain is observed for

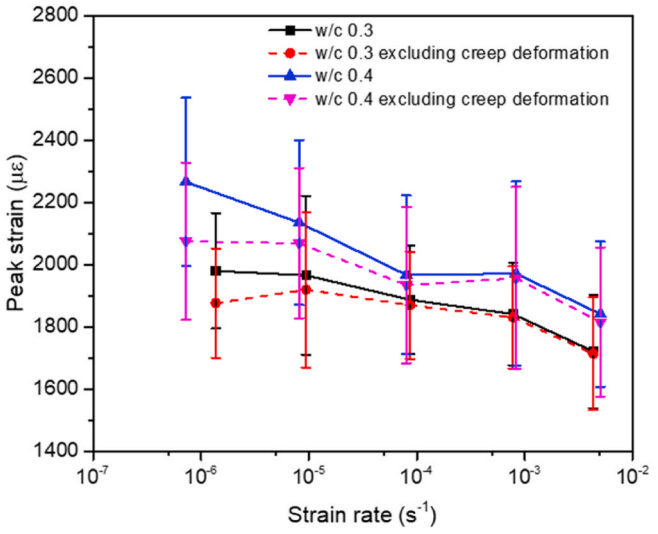

Fig. 13. The variation of peak strain with the strain rate.

both w/c ratios in the investigated strain rate range. The degree of decline is more pronounced for samples with w/c ratio of 0.4. This observed trend is likely to be the consequence of less viscoelastic and non-reversible deformation with the increasing strain rate [24–26,39–41]. The peak strains excluding the linear creep deformation during loading process are also presented in Fig. 13 (dash line). Again, since the possible non-linear creep deformation is not considered in the current work, the even lower value of non-creep peak strain could be expected for the slow strain rate tests. It can be seen from Fig. 13 that the creep effect dominates the strain rate sensitivity of the peak strain at the low and moderate strain rates ($<10^{-3}$/s). However, a continuous decrease of peak strain is observed at higher strain rate, where the creep is unlikely to play a role. Therefore, it may be attributed to the less generated non-reversible deformation during the loading process. In literature, there are relatively few studies focusing on the rate-dependent peak strain under flexural loading. Nevertheless, according to the compressive tests on concrete conducted by Pan and Weng [40], the peak strain generally decreases with the increasing strain rate ranging from 5×10^{-6}/s to 1×10^{-1}/s. However, Harsh et al. [39] found that the peak strain of cement paste and mortar in compression first decreases and then increases with increasing strain rate. In their study, the turning point for cement paste is in between around 3×10^{-4}/s and 3×10^{-3}/s. The author claimed that this further increase in peak strain might be the result of limitations in crack velocity compared to the rate of loading [39]. In contrast, Sun et al. [41] reported that the strain rate has little effect on the peak strain of concrete under compression. It seems that there is no consensus yet regarding the effect of strain rate on the peak strain in the current literature [2,39–42].

3.5. Fracture surface

It has been reported that the cracking path of cementitious materials is also sensitive to the strain rate [10]. To gain more information about the possible morphological changes of the fracture surface as a result of different loading rates, some of the fractured MCBs were examined using secondary electron (SE) and backscattered electron (BSE) modes in an ESEM. The surface morphology can be observed in the SE mode, while the BSE mode yields the information on the distribution of phases. Several beams were also examined using the XCT technique. It should be noted that due to the highly heterogeneous microstructure of cement paste at the microscale, a notable distinction of fracture surfaces between the successive strain rate tests can hardly be identified. This is also demonstrated by the small difference in mechanical properties between the successive strain rates. Therefore, only the fracture surfaces of

samples (w/c 0.3) under the slowest and fastest strain rate were compared here. For each strain rate, more than eight fractured samples were examined in the ESEM. In addition, four beams were scanned using XCT before and after failure. Fig. 14 shows the typical SE and BSE images of the fracture surfaces for the two strain rates. Note that for the flexural failure the critical crack is most likely to initiate and propagate at the tensile zone of the cross-section. Therefore, particular attention was paid on this area (red box in Fig. 14). Fig. 15 compares the XCT obtained fracture profiles for the MCBs under the slowest and fastest strain rates. It is known that at the microscale the cement paste mainly comprises calcium silicate hydrates (C–S–H), calcium hydroxide (CH), anhydrous cement particles and pores. Moreover, two forms of C–S–H, namely inner and outer hydration products (or high-density and low-density C–S–H), are generally identified [43–45]. It can be seen from Fig. 14 that a higher content of unhydrated cement particles is exposed in the tensile zone for the highest strain rate compared to the lowest strain rate. For quantification, in total 16 fractured surfaces of w/c 0.3 samples were examined for both strain rates. The calculated average ratio of total exposed cement particle area (in tensile zone) to the area of tensile zone is 6.34 ± 2.01% for the lowest strain rate (1.3 με/s) and 9.60 ± 3.81% for the highest strain rate (4341.7 με/s). This indicates that more inner hydration products surrounding the clinker are fractured at higher strain rate. This is also observed in the XCT results between the slowest and fastest strain rates (see Fig. 15). By using the higher magnification of microscopy, Jawed et al. [46] found that the fracture of CH is also more common at higher strain rate. This is somewhat analogous to the fracture of concrete samples loaded at higher strain rate [5,10,13,14,47], in which the crack tends to pass through the aggregate instead of following the mortar-aggregate interfaces as typically happens at low strain rates. Furthermore, one has to notice that the inner and outer hydration products are not completely homogeneous [48,49]. In fact, they both contain a wide gradient of material properties [16]. Therefore, it can be assumed that with the increasing strain rate, the cracking path may gradually shrift to stronger phases in hydration products, which results in the increase of strength. However, it is necessary to mention that more microscopic images and XCT tests may be needed to confirm this observation at the microscale.

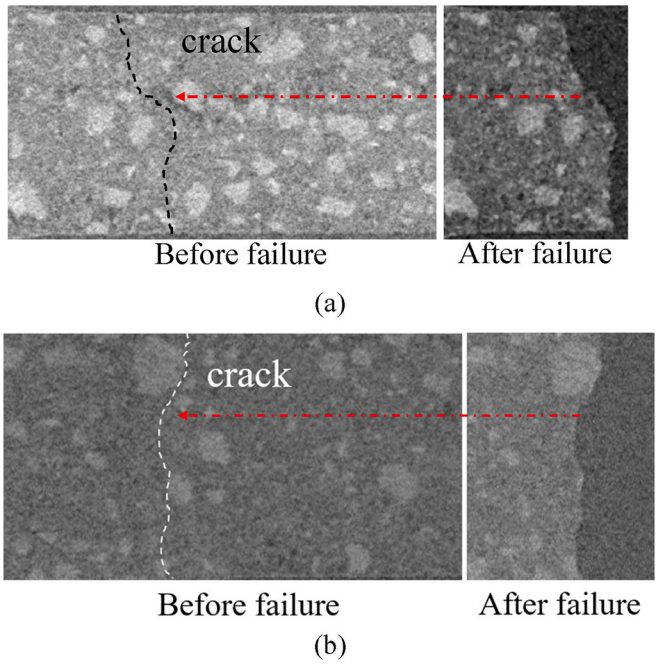

Fig. 15. The comparison of XCT obtained fracture profile for the MCBs with w/c 0.3 under (a) the slowest strain rate and (b) the fastest strain rate. (The crack path in the left picture is defined by the fracture profile in the right picture).

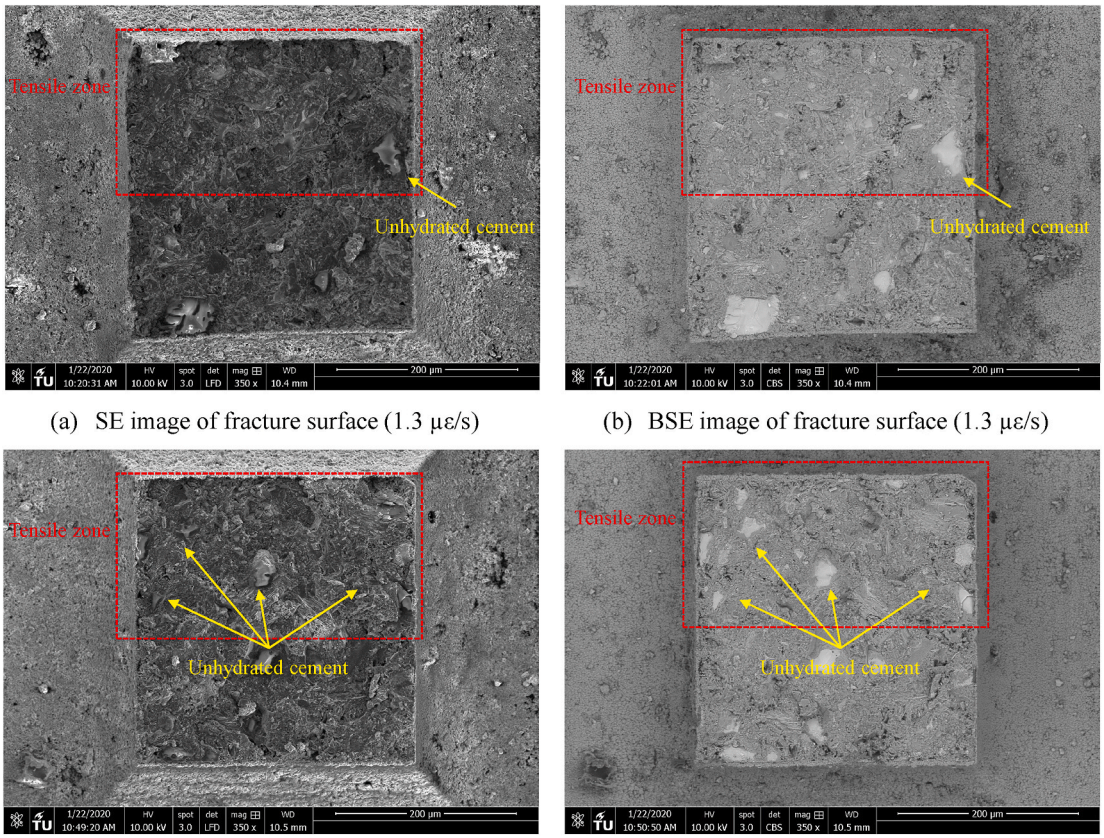

(a) SE image of fracture surface (1.3 με/s) (b) BSE image of fracture surface (1.3 με/s)

Fig. 14. The typical microscopy of fracture surface for the sample with w/c 0.3.

In addition, it has been reported that the cracking paths of cementitious materials become less tortuous at higher strain rate [5,10,47]. Unfortunately, the quantitative measurement regarding the roughness of fracture surface is not available in current study but will be performed in future research.

4. Discussion

In this section, several existing mechanisms are used to explain the rate-dependent behaviour of cement paste at microscale. Attempts to gain new insights are also made. It is generally argued that the inertia effect and rate-dependent crack propagation become significant only at very high strain rate, e.g. at least more than 1/s [7,9,28]. Since in this study the strain rates are lower than 1/s, these effects are not taken into account. Several other mechanisms, e.g. creep effect and Stéfan effect, may occur simultaneously in the low and intermediate strain rates. It is important to address their dominances at certain strain rate range [9]. In addition, since the size effect of strength is a well-known phenomenon for cementitious materials [21,50–52], it would be interesting to compare the microscale tests with the macroscopic tests results. Therefore, the comparison of strain rate sensitivity in terms of dynamic increasing factor (DIF) with macroscopic experimental results is also presented in Section 4.2.

4.1. Possible mechanisms for the strain rate sensitivity of cement paste at microscale

4.1.1. Creep effect

In the current work, five strain rates were investigated and they can be roughly classified into two groups: one group with strain rate lower than 10^{-3}/s and the other one is higher than 10^{-3}/s. In the latter strain rate group, the test durations are less than 3 s. Therefore, it is not difficult to assume that the creep, including both linear and non-linear creep, plays an insignificant role in the strain rate sensitivity of the mature cement paste within this short duration. By contrast, the viscoelastic effect on the apparent elastic modulus in the first strain rate group has been clearly demonstrated in Section 3.3. This spurious rate-dependency of the apparent elastic modulus is thought to be mainly caused by the development of viscoelastic deformations during the slow loading process at the stress level of 40%–60%. It can also be expected that higher w/c ratio leads to more creep deformation and thus higher reduction of apparent elastic modulus [9,12,33,53]. Regarding the strain rate sensitivity of strength, some researchers [9,10,39] suggest that the creep effect is the main governing effect at low and intermediate strain rate ($<10^{-1}$/s). Fischer et al. [9] carried out compressive tests on 2-day-old cement paste in the strain rate range of 10^{-6}/s to 10^{-2}/s and claimed that the increased test duration allows for the development of more nonlinear creep-related damage. This statement is mainly based on the experimental observations in the interesting work of Rossi et al. [37], in which a good correlation between the number of measurable acoustic events and the creep strain is found for the compressive creep of mature concrete at stress level more than 54% of strength. The author then proposed that the basic creep of the concrete is mainly related to the microcracking which induces additional self-drying shrinkage under stress [37]. Therefore, the reduction of material strength with a lower strain rate is suggested to be re-interpreted as the consequence of more accumulated creep related damage, i.e. microcracking [9]. Note that this so-called creep related damage is only significant at high stress level, i.e. at least more than 40% of compressive strength in macroscopic tests [9]. In the case of the current study, more than 70% of strength is expected to exhibit significant creep related damage [36]. In consideration of the influence of w/c ratio on the strain rate sensitivity of strength, based on the previous evidences, it can be anticipated that at a low strain rate range the higher w/c ratio should generate a higher extent of creep related damage and thus lead to higher reduction of strength. This is consistent with the experimental results in Section 3.2. These results further confirm that in the low loading tests the strain rate sensitivity of cement paste is mainly affected by the creep.

4.1.2. Stéfan effect and fracture process

Another possible physical mechanism related to the strain rate sensitivity is the well-known Stéfan effect. The application of this theory in cementitious materials was first introduced by Rossi [13]. This effect can be briefly described as follows: when a thin film of a viscous liquid, e.g. water, is trapped between two plane and parallel plates that are separated at a certain velocity, the film will exert an opposing force on the plates. This opposing force is dependent on the velocity of separation, the distance between two plates and also the viscosity and volume of the liquid. When it comes to cementitious materials, it is suggested that the faster loading rate, the higher content of free water and the finer pores will all result in the higher force on the walls of gel and capillary pores [13]. These forces act as the prestresses on the walls of pores and thus prevent the cracking to some extent. Bearing this Stéfan effect in mind, several experimental observations in the current study can be properly explained. It is easy to understand that for cement paste loaded at low strain rates the cracks preferentially initiate and propagate at the weak spots (e.g. capillary and gel pores) or locations where stress concentration is most likely to occur (e.g. the crack tip and the interface between the clinker and hydration product). However, with the increasing strain rate, the presence of water in these weak spots may enhance their strengths due to the Stéfan effect. It is possible that the strength of weak spots might reach the strength of inner product or even CH provided that the strain rate is high enough [13,46]. This leads to a greater homogeneity of the cement paste, so that the crack is likely to pass through these phases alike. This is probably one of the reasons for more fractures of the aggregate and less tortuous cracking path observed in most concrete samples under high strain rate loading [5,10,13,47]. To be more specific, the Stéfan effect on the fracture of cement paste at microscale might be twofold: at low strain rate the microcracks generally develop in a diffuse manner at first and are randomly distributed inside the cement paste. The Stéfan effect might delay the diffusing of microcracks at higher strain rate. This explains the experimental observations in Section 3.1 and 3.3, where less and delayed pre-peak nonlinearity as well as greater elastic moduli were found at higher strain rate. Secondly, the Stéfan effect may also counteract the localization of microcracks before failure. As a result, higher global strength of cement paste is obtained.

It is still worth noting that in the current work the Stéfan effect is believed to become significant compared to the creep effect when the strain rate is higher than 10^{-3}/s. This is clearly manifested in the increase of both elastic modulus and strength at the strain rate more than 10^{-3}/s, where the creep effect is thought to be negligible. It is also found that in this strain rate range both the increased percentage and absolute value of strength tends to be greater for the lower w/c ratio, which is in contrast to the trend observed in the low strain rate range. A possible explanation may be that the mature cement paste with lower w/c ratio has higher volumetric contents of inner hydration product [44,54], which contains finer pores than the outer hydration product. If the crack passes through the hydration products, the larger the content of inner products, the stronger the Stéfan effect will be. Note that this explanation is based on the assumption that the Stéfan effect also applied to very small pores [7,13]. Hence, the strain rate sensitivity of cement paste is thought to be more significant in lower w/c ratio at higher strain rate. Similar trend has also been observed in the macroscopic tests on mortar at strain rate more than 2.7×10^{-4}/s [31]. However, it should be stressed that since the results of cement paste at the microscale show high scatter and only two w/c ratios were investigated in the current study, it is difficult to draw a firm conclusion based on the limited data. Therefore, more experimental confirmations would be necessary.

To sum up, the rate-dependency of cement paste is thought to be dominated by the creep effect at low strain rate, while for higher strain rate the Stéfan effect seems to be the governing factor. It is interesting to

note that the movement and distribution of free water inside the cement paste appear to be the critical parameters in both cases. On the one hand, the water seems to have a negative effect by reducing the intrinsic strength of cement paste at low strain rates due to the creep effect. On the other hand, the water plays an important role in the enhancement of strength due to the Stéfan effect at higher strain rates. Both effects are believed to contribute to the strain rate sensitivity behaviour of cement paste. Nevertheless, further studies regarding the effect of moisture content on the strain rate sensitivity of cement paste at microscale may be needed.

4.2. Comparison with macroscopic tests

The dynamic increase factor (DIF), defined as the ratio between the dynamic and static strength, has been commonly used to quantify the rate-dependence of cementitious material. It has been extensively investigated by many researchers and various approximate empirical formulas have been proposed [47,55,56]. In this section, the average DIF was used to compare the results of MCB bending tests with that of macroscopic tests in literature [6,9,11,31,39,41,42,47,55,57–59]. Normally, a reference strength at a certain strain rate should be chosen to normalize the DIF. Herein, we consider the strength at strain rate of 10^{-6}/s as the reference strength. It has to be noted that most of past researches focused on the mortar and concrete samples, while the available data for cement paste under flexural loading are very scarce. Even though the study of Chen et al. [60] demonstrated that the strain rate effects on paste, mortar and concrete are in general similar, the comparison between different material compositions should still be interpreted with caution due to the complexity of the rate-dependent behaviour.

Fig. 16 shows the comparison of DIF obtained in the current study and the macroscopic tests on cement paste, mortar and concrete. It can be seen from Fig. 16 that in general the all DIF results exhibit a similar trend with some discrepancies. These discrepancies are mainly attributed to the variations in loading conditions, material compositions and the moisture content. In consideration of the testing method, it has been reported that the strain rate sensitivity of flexural strength is in between that of tensile strength and compressive strength while the strain rate sensitivity of tensile strength is the most pronounced [5,11,47]. In Fig. 16, at a given strain rate the DIF obtained in current work is slightly lower than most macroscopic results even including the results of cement paste in compression. This slight difference seems to suggest a size-effect of DIF. However, the results should be interpreted with caution. Since most of macroscopic samples were tested just after curing and were exposed to the ambient RH [6,11,31,39,55,57–59]. There is always moisture remaining inside the samples during the tests, as it normally takes days or longer (depending on the specimen size) for internal RH of regular size sample to equilibrate with the environment [61]. This is definitely not the case in the current study because the MCB quickly equilibrated to the ambient RH before the test due to the extremely thin cross-section [36]. Therefore, based on the assumptions in previous sections, the lower content of water in MCB might be the reason for the lower value of DIF. Nevertheless, further evidence on this aspect may be required. In this study, the overall difference of DIF between the microscale and macroscale tests is not as evident as the size-effect of strength [21,52]. This is similar with the findings in other researches [51,62] that the strain rate sensitivity of cementitious materials in terms of DIF is found to be not significantly affected by the specimen size.

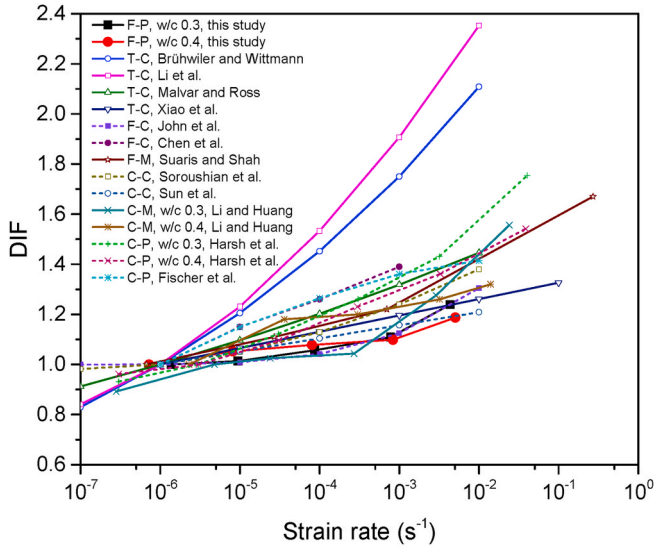

Fig. 16. The comparison of DIF between the microscopic and macroscopic results (The first letter represents the testing method, i.e. 'F' for flexural, 'T' for tensile and 'C' for compressive; the second letter denotes the sample type, i.e. 'P' for paste, 'M' for mortar and 'C' for concrete.).

One has to notice that it is also important to consider local differences of samples in microscopic tests. The current adopted "averaging" approach is useful in a sense that it enables to qualitatively and, to a certain extent, quantitatively compare the results from microscopic tests to trends reported in the published literature (mainly macroscopic tests). Future work should focus on the assessment of the local difference by combining the experimentally obtained microstructure (e.g. CT scan) with the fracture model (e.g. the lattice model). In this way, it is possible to directly reveal the local differences between individual samples and evaluate their mechanical properties at the same time.

5. Conclusion

In this paper, the micro-cantilever bending tests were used to investigate the strain rate sensitivity of mechanical properties of cement paste at the microscale. Two w/c ratios and five different strain rates ranging from 10^{-6}/s to 10^{-2}/s were tested. The following conclusions can be drawn from the experimental results:

(1) The tests confirm that the mechanical properties of cement paste are sensitive to the strain rate. The flexural strength and the elastic modulus of cement paste increase with increasing strain rate, while the peak strain exhibits the opposite trend.
(2) The stochastic aspect of flexural strength was evaluated using the Weibull distribution. It is found that the Weibull modulus is independent of the strain rate in current study.
(3) At low strain rate, i.e. $<10^{-3}$/s, the stress-strain curves show less and earlier pre-peak nonlinearity with increasing strain rate. By using the Boltzmann's superposition principle to interpret the deformation during the loading process, it was found that the rate-dependency of elastic modulus is mainly caused by the viscoelastic effect. In addition, the creep-related damage at higher stress level is believed to result in the reduction of strength. It is then concluded that the creep effect might play a dominant role in the strain rate sensitivity of cement paste at low strain rate range.
(4) At higher strain rate, i.e. $>10^{-3}$/s, the examination of fracture surfaces suggests that with increasing strain rate there is a transition of cracking path to stronger phases, such as inner hydration products and CH. Since the creep effect is almost negligible in this strain rate range, these observations imply that the Stéfan effect could give rise to strain rate sensitivity of cement paste at higher strain rate range.
(5) Based on the comparison of DIF obtained in microscale tests and macroscale tests, it seems that the strain rate sensitivity is not significantly affected by the specimen size.

(6) The two mechanisms, i.e. creep and Stéfan effect, can properly explain the experimental observations in this study. It is therefore suggested that the role of water is the primary reason for the strain rate sensitivity of cementitious material. Further studies regarding the effect of moisture content on rate-dependent mechanical properties at microscale are needed.

Declaration of competing interest

The authors declare that they have no known competing financial interests or personal relationships that could have appeared to influence the work reported in this paper.

Acknowledgments

Yidong Gan would like to acknowledge the funding supported by China Scholarship Council under grant number 201706130140. Claudia Romero Rodriguez acknowledges the financial support from the Construction Technology Research Program funded by the Ministry of Land, Infrastructure and Transport of the Korean Government under the grant 17SCIP-B103706-03. Mr. Arjan Thijssen is also gratefully acknowledged for his help with the ESEM experiments.

References

[1] M. Belaoura, Compressive behaviour of concrete at high strain rates, Mater. Struetures. (1991) 425–450.
[2] J. Xiao, L. Li, L. Shen, C.S. Poon, Compressive behaviour of recycled aggregate concrete under impact loading, Cement Concr. Res. 71 (2015) 46–55.
[3] L.J. Malvar, C.A. Ross, Review of strain rate effects for concrete in tension, ACI Mater. J. 95 (1998) 735–739.
[4] J.H. Yon, N.M. Hawkins, A.S. Kobayashi, Strain-rate sensitivity of concrete mechanical properties, ACI Mater. J. 89 (1992) 146–153.
[5] S. Wu, X. Chen, J. Zhou, Tensile strength of concrete under static and intermediate strain rates: correlated results from different testing methods, Nucl. Eng. Des. 250 (2012) 173–183.
[6] W. Suaris, S.P. Shah, Properties of concrete subjected to impact, J. Struct. Eng. 109 (1983) 1727–1741.
[7] P. Rossi, F. Toutlemonde, Effect of loading rate on the tensile behaviour of concrete: description of the physical mechanisms, Mater. Struct. Constr. 29 (1996) 116–118.
[8] A.S. Agar Ozbek, R.R. Pedersen, J. Weerheijm, K. van Breugel, Mesoscopic modeling of the impact behavior and fragmentation of porous concrete, Cem. Concr. Compos. 102 (2019) 116–133.
[9] I. Fischer, B. Pichler, E. Lach, C. Terner, E. Barraud, F. Britz, Compressive strength of cement paste as a function of loading rate: experiments and engineering mechanics analysis, Cement Concr. Res. 58 (2014) 186–200.
[10] Z.P. Bazant, R. Gettu, Rate effects and load relaxation in static fracture of concrete, ACI Mater. J. 89 (1992) 457–468.
[11] R. John, S.P. Shah, Y.S. Jeng, A fracture mechanics model to predict the rate sensitivity of mode I fracture of concrete, Cement Concr. Res. 17 (1987) 249–262.
[12] S. Liang, Y. Wei, X. Gao, Strain-rate sensitivity of cement paste by microindentation continuous stiffness measurement: implication to isotache approach for creep modeling, Cement Concr. Res. 100 (2017) 84–95.
[13] P. Rossi, A physical phenomenon which can explain the mechanical behaviour of concrete under high strain rates, Mater. Struct. 24 (1991) 422–424.
[14] I. Vegt, K. Van Breugel, J. Weerheijm, Failure mechanisms of concrete under impact loading, Proc. 6th Int. Conf. Fract. Mech. Concr. Concr. Struct. - Fract. Mech. Concr. Concr. Struct. 1 (2007) 579–587.
[15] H. Zhang, B. Šavija, S.C. Figueiredo, E. Schlangen, Experimentally validated multi-scale modelling scheme of deformation and fracture of cement paste, Cement Concr. Res. 102 (2017) 175–186.
[16] H. Zhang, B. Šavija, M. Luković, E. Schlangen, Experimentally informed micromechanical modelling of cement paste: an approach coupling X-ray computed tomography and statistical nanoindentation, Compos. B Eng. 157 (2019) 109–122.
[17] H. Zhang, Y. Xu, Y. Gan, Z. Chang, E. Schlangen, B. Šavija, Combined experimental and numerical study of uniaxial compression failure of hardened cement paste at micrometre length scale, Cement Concr. Res. 126 (2019).
[18] H. Zhang, B. Šavija, E. Schlangen, Towards understanding stochastic fracture performance of cement paste at micro length scale based on numerical simulation, Construct. Build. Mater. 183 (2018) 189–201.
[19] B. Šavija, H. Zhang, E. Schlangen, Micromechanical testing and modelling of blast furnace slag cement pastes, Construct. Build. Mater. 239 (2020).
[20] H. Zhang, Y. Gan, Y. Xu, S. Zhang, E. Schlangen, B. Šavija, Experimentally informed fracture modelling of interfacial transition zone at micro-scale, Cement Concr. Compos. 104 (2019), 103383.
[21] H. Zhang, B. Šavija, Y. Xu, E. Schlangen, Size effect on splitting strength of hardened cement paste: experimental and numerical study, Cement Concr. Compos. 94 (2018) 264–276.
[22] Y. Gan, H. Zhang, B. Šavija, E. Schlangen, K. van Breugel, Static and fatigue tests on cementitious cantilever beams using nanoindenter, Micromachines 9 (2018).
[23] H. Zhang, B. Šavija, E. Schlangen, Combined experimental and numerical study on micro-cube indentation splitting test of cement paste, Eng. Fract. Mech. 199 (2018) 773–786.
[24] J. Cao, D.D.L. Chung, Effect of strain rate on cement mortar under compression, studied by electrical resistivity measurement, Cement Concr. Res. 32 (2002) 817–819.
[25] G. Cusatis, Strain-rate effects on concrete behavior, Int. J. Impact Eng. 38 (2011) 162–170.
[26] H. Su, J. Hu, J. Tong, Z. Wen, Rate effect on mechanical properties of hydraulic concrete flexural-tensile specimens under low loading rates using acoustic emission technique, Ultrasonics 52 (2012) 890–904.
[27] I. Vegt, R.R. Pedersen, L.J. Sluys, J. Weerheijm, Modelling of impact behaviour of concrete-an experimental approach, Comput. Model. Concr. Struct. (2006) 451–458.
[28] H.W. Reinhardt, J. Weerheijm, Tensile fracture of concrete at high loading rates taking account of inertia and crack velocity effects, Int. J. Fract. 51 (1991) 31–42.
[29] R.R. Pedersen, A. Simone, M. Stroeven, L.J. Sluys, Mesoscopic modelling of concrete under impact, Proc. 6th Int. Conf. Fract. Mech. Concr. Concr. Struct. - Fract. Mech. Concr. Concr. Struct. 1 (2007) 571–578.
[30] J. Zhang, G.W. Scherer, Comparison of methods for arresting hydration of cement, Cement Concr. Res. 41 (2011) 1024–1036.
[31] L. Zhaoxia, H. Yaoping, Effect of strain rate on the compressive strength surface cracking and failure mode of mortar, ACI Mater. J. 95 (1998) 512–518.
[32] B. Zech, F.H. Wittmann, Variability and mean value of strength of concrete as function of load, J. Am. Concr. Inst. 77 (1980) 358–362.
[33] M. Irfan-Ul-Hassan, B. Pichler, R. Reihsner, C. Hellmich, Elastic and creep properties of young cement paste, as determined from hourly repeated minute-long quasi-static tests, Cement Concr. Res. 82 (2016) 36–49.
[34] L. Su, Y. feng Wang, S. qi Mei, P. fei Li, Experimental investigation on the fundamental behavior of concrete creep, Construct. Build. Mater. 152 (2017) 250–258.
[35] d L. Reiss, EdwarM.E. Gurtin, E. Sternberg, On the linear theory of viscoelasticity, Arch. Ration. Mech. Anal. 7 (1961) 402–411.
[36] Y. Gan, M. Vandamme, H. Zhang, Y. Chen, E. Schlangen, Micro-cantilever testing on the short-term creep behaviour of cement paste at micro-scale, Cement Concr. Res. 134 (2020).
[37] P. Rossi, J.L. Tailhan, F. Le Maou, L. Gaillet, E. Martin, Basic creep behavior of concretes investigation of the physical mechanisms by using acoustic emission, Cement Concr. Res. 42 (2012) 61–73.
[38] Z. Hu, A. Hilaire, J. Ston, M. Wyrzykowski, P. Lura, K. Scrivener, Intrinsic viscoelasticity of C-S-H assessed from basic creep of cement pastes, Cement Concr. Res. 121 (2019) 11–20.
[39] S. Harsh, Z. Shen, D. Darwin, Strain-rate sensitive behavior of cement paste and mortar in compression, ACI Mater. J. 87 (1990) 508–516.
[40] H.H. Pan, G.J. Weng, Study on strain-rate sensitivity of cementitious composites, J. Eng. Mech. 136 (2010) 1076–1082.
[41] J.S. Sun, L.J. Ma, Y.M. Dou, J. Zhou, Effect of strain rate on the compressive mechanical properties of concrete, Adv. Mater. Res. 450–451 (2012) 244–247.
[42] S. Xiao, H. Li, P.J.M. Monteiro, Influence of strain rates and load histories on the tensile damage behaviour of concrete, Mag. Concr. Res. 62 (2010) 887–894.
[43] P.D. Tennis, H.M. Jennings, A model for two types of calcium silicate hydrate in the microstructure of Portland cement pastes, Cement Concr. Res. 30 (2000) 855–863.
[44] G. Constantinides, F.J. Ulm, The effect of two types of C-S-H on the elasticity of cement-based materials: results from nanoindentation and micromechanical modeling, Cement Concr. Res. 34 (2004) 67–80.
[45] J.H. Taplin, A method for following the hydration reaction in portland cement paste, Aust. J. Appl. Sci. 10 (1959) 329–345.
[46] I. Jawed, G. Childs, A. Ritter, S. Winzer, T. Johnson, D. Barker, High-strain-rate behavior of hydrated cement pastes, Cement Concr. Res. 17 (1987) 433–440.
[47] X. Chen, S. Wu, J. Zhou, Y. Chen, A. Qin, Effect of testing method and strain rate on stress-strain behavior of concrete, J. Mater. Civ. Eng. 25 (2013) 1752–1761.
[48] M. Vandamme, F.J. Ulm, Nanogranular origin of concrete creep, Proc. Natl. Acad. Sci. U.S.A. 106 (2009) 10552–10557.
[49] C. Hu, Z. Li, A review on the mechanical properties of cement-based materials measured by nanoindentation, Construct. Build. Mater. 90 (2015) 80–90.
[50] A. Carpinteri, A. Spagnoli, A fractal analysis of size effect on fatigue crack growth, Int. J. Fatig. 26 (2004) 125–133.
[51] V. Bindiganavile, N. Banthia, Size effects and the dynamic response of plain concrete, J. Mater. Civ. Eng. 18 (2006) 485–491.
[52] Z.P. Bažant, Size effect in blunt fracture: concrete, rock, metal, J. Eng. Mech. 110 (1984) 518–535.
[53] M. Vandamme, F.J. Ulm, Nanoindentation investigation of creep properties of calcium silicate hydrates, Cement Concr. Res. 52 (2013) 38–52.
[54] J.J. Thomas, H.M. Jennings, A.J. Allen, The surface area of cement paste as measured by neutron scattering: evidence for two C-S-H morphologies, Cement Concr. Res. 28 (1998) 897–905.
[55] >R.C. Malvar LJ, Review of strain rate effects for concrete in tension, Am. Concr. Institud. Mater. J. (1998) 735–739.
[56] H.C. Fu, M.A. Erki, M. Seckin, Review of effects of loading rate on reinforced concrete, J. Struct. Eng. 117 (1991) 3660–3679.

[57] P. Soroushian, K.B. Choi, A. Alhamad, Dynamic constitutive behavior of concrete, J. Am. Concr. Inst. 83 (1986) 251–259.
[58] Li Qingbin, Zhang Chuhan, Wang Guanglun, Dynamic damage constitutive model of concrete in uniaxial tension, Eng. Fract. Mech. 53 (1996) 449–455.
[59] E. Brühwiler, F.H. Wittmann, Failure of dam concrete subjected to seismic loading conditions, Eng. Fract. Mech. 35 (1990) 565–571.
[60] X. Chen, S. Wu, J. Zhou, Experimental and modeling study of dynamic mechanical properties of cement paste, mortar and concrete, Construct. Build. Mater. 47 (2013) 419–430.
[61] J.A. Almudaiheem, W. Hansen, Effect of specimen size and shape on drying shrinkage of concrete, ACI Mater. J. 84 (1987) 130–135.
[62] D.Y. Yoo, N. Banthia, Size-dependent impact resistance of ultra-high-performance fiber-reinforced concrete beams, Construct. Build. Mater. (2017).
[63] Y. Gan, C. Rodriguez, H. Zhang, E. Schlangen, K. van Breugel, B. Šavija, Modeling of microstructural effects on the creep of hardened cement paste using an experimentally informed lattice model, Comput. Civ. Infrastruct. Eng. (2021) 1–17.
[64] Y. Gan, H. Zhang, Y. Zhang, Y. Xu, E. Schlangen, K. van Breugel, B. Šavija, Experimental study of flexural fatigue behaviour of cement paste at the microscale, Int. J. Fatigue. (2021). In press.
[65] Y. Gan, M. Vandamme, Y. Chen, E. Schlangen, K. van Breugel, B. Šavija, Experimental investigation of the short-term creep recovery of hardened cement paste at micrometre length scale, Cement Concr. Res. (2021). Submitted for publication.